

Towards Precision Biocatalysis - Leveraging Inline NMR for Autonomous Experimentation in Flow Reactors

Felix Ott,^[a] Gudrun Gygli,^[a] Kersten S. Rabe,^[a] and Christof M. Niemeyer^{*[a]}

Reactor automation is a transformative force for chemical processes, but the potential of reaction monitoring for machine-assisted autonomous biocatalytic reaction optimization is still largely unexplored. To address this gap, we report on automated reactor optimization for biocatalytic flow-through microreactors. For this purpose, the inline NMR analysis of an enzymatically catalyzed stereoselective reduction of a prochiral diketone was combined with a self-developed open-source analysis and control software. The algorithm is continuously fed with spectra from a benchtop NMR instrument

acquired from a reaction solution from a microreactor filled with biocatalytically active materials and adjusts the flow rate of the pumps to achieve predetermined target concentrations of the product. We show that through this automated coupling of data analysis and process parameterization, for example, maximum conversion efficiency can be achieved for a given bioreactor. This work illustrates the potential of inline NMR reaction monitoring for biocatalytic processes and provides a starting point for innovation to develop automated processes for precision biocatalysis through integrated data analysis.

Introduction

Reactor automation is transforming the discovery and development of chemical processes by delegating repetitive tasks such as experimentation and data collection to machines, allowing researchers to focus on critical interpretation and creative problem solving.^[1] Robotic platforms for batch and continuous flow processes are becoming more versatile and allow access to a wider range of chemical processes, even for autonomous multi-step synthesis.^[2] Here, advances in process analytics enable real-time monitoring of reactions, accelerate data acquisition, improve process control for safety and quality, and, by integrating these tools into the control software, enable feedback loops for adaptive multi-step screening and self-optimization.^[1–3] While a high degree of machine-assisted automation is now well established in pure and applied chemistry,^[4,5,6] it is less prevalent in industrial biocatalysis, which is widely regarded as a “game changer” for developing a sustainable economy.^[7–10] The proven benefits of biocatalytic processes and the vast array of available enzymes offer the potential for sustainable “green” production of valuable molecules, such as high-value products like pharmaceutical active ingredients.^[9,11–13] To address the main challenges in advancing

this field - such as developing enzyme cascades, standardizing production processes, and implementing continuous process technology,^[13] the concept of flow biocatalysis has gained significant attention.^[14–19] Flow biocatalysis adapts the core principles of flow chemistry, where machine-assisted modular chemical synthesis is continuous and compartmentalized in miniaturized reactors, to meet the specific requirements of biocatalysis. For this purpose, large quantities of enzyme biocatalysts must be immobilized in microstructured flow reactors under gentle conditions. This can be achieved with “all-enzyme hydrogels” (AEH) formed by the self-assembly of SpyCatcher (SC)/SpyTag (ST)-mediated site-specific enzyme conjugation, resulting in biocatalytic materials that consist almost entirely of enzymes and thus make optimal use of the available reaction space.^[20–22]

In terms of autonomous experimentation, flow biocatalysis as well as flow chemistry, requires precise analytics in real time that can be realized online (instrument with bypass) and inline (instrument directly in the analyte stream),^[23] to enable robust process control and data for the creation of models for automated process optimization. Real-time monitoring allows for immediate adjustments to reaction conditions, which is crucial for biocatalytic systems that may lack long-term stability and exhibit complex, unpredictable behavior.^[24] Techniques like HPLC, GC, UV-Vis, IR, Fluorescence, Raman, and NMR spectroscopy can be used for reaction monitoring.^[25] While the best technique depends on the specific reaction, NMR stands out for its versatility, providing structural information, quantitative data, and being non-destructive. The emergence of affordable benchtop NMR instruments makes this method especially appealing for research groups, and it has already been employed for monitoring and optimizing flow reactions.^[26–29]

However, benchtop NMR has rarely been used for reaction monitoring in biocatalytic processes. Farley *et al.* used an inline setup combining benchtop NMR and IR to monitor the kinetic resolution step of a lipase-catalyzed transesterification,^[30] while

[a] Institute for Biological Interfaces 1 (IBG-1), Karlsruhe Institute of Technology, Eggenstein-Leopoldshafen, Germany

Correspondence: Prof. Dr. Christof M. Niemeyer, Institute for Biological Interfaces 1 (IBG-1), Karlsruhe Institute of Technology, Hermann-von-Helmholtz Platz 1, 76344 Eggenstein-Leopoldshafen, Germany.
Email: niemeyer@kit.edu

Supporting Information for this article is available on the WWW under <https://doi.org/10.1002/cmt.202400049>

© 2024 The Author(s). Chemistry - Methods published by Chemistry Europe and Wiley-VCH GmbH. This is an open access article under the terms of the Creative Commons Attribution License, which permits use, distribution and reproduction in any medium, provided the original work is properly cited.

Legner *et al.* used immobilized lipase in a cartridge reactor for hydrolysis followed by online-monitored esterification.^[31] More recently, Claaßen *et al.* used an online setup to monitor the two-step biocatalytic synthesis of aromatic aminoalcohols in aqueous media.^[32] Very recently, Schmidt *et al.* reported on the analysis of a batch reaction of a diastereoselective enzymatic α -amino acid synthesis, which was quantified by a benchtop NMR.^[33] While these seminal papers focused on analytically characterizing the progress of reaction, to the best of our knowledge, there have been no reports of utilizing online monitoring for machine-assisted autonomous biocatalytic reaction optimization. Here, we present the utilization of inline NMR for autonomously enhancing the biocatalytic synthesis of chiral alcohols (Figure 1), addressing a common challenge in flow biocatalysis where reactor efficiency diminishes over prolonged reaction durations. With the automatic adjustment of the critical parameter flow rate based on a benchtop NMR spectrometer, complemented by an open-source analysis and control software, this proof-of-concept study is intended to serve for future innovations towards precision biocatalysis.

Results and Discussion

To establish an NMR-based reaction monitoring system, we chose the well-studied model reduction of prochiral 5-nitrononane-2,8-dione (NDK, **1**), whose two carbonyl groups can be reduced by the NADPH-dependent alcohol dehydrogenase

LbADH to form 8-hydroxy-5-nitrononane-2-one (HK, **2**) and finally the chiral 5-nitrononane-2,8-diol (diol **3**) (Figure 1a).^[20,21,22,34,35] The regeneration of the cofactor NADPH is carried out by the glucose dehydrogenase BsGDH using glucose as a sacrificial substrate. NAD(P)H-dependent oxidoreductases are of great interest to the chemical industry.^[36] To investigate the suitability of benchtop NMR for the analysis of NDK reduction, we first performed analyses with isolated educt **1**, hydroxyketone intermediate **2** and diol product **3** using an 80 MHz benchtop NMR instrument (Spinsolve 80 Ultra Carbon, Magritek). The NMR spectra showed that the CH₂ protons in alpha position to the carbonyl group (highlighted in blue, in Figure 1a,b) and the CH₃ protons in beta position to the formed hydroxyl group (orange) yielded sufficiently isolated signals to determine the change in the amounts of alcohol or ketone, respectively, in the sample tube when 3-(trimethylsilyl)propionic acid-2,2,3,3-d₄ (TMSP-d₄, green labeled signals in Figure 1a,b) was used as an internal standard. For a complete spectrum of the intermediate hydroxyketone **2**, see Figure S1, Supporting Information. In addition, NMR signal acquisition parameters were optimized to determine the T₁ times of the monitored signals, the strength of the pre-saturation power required to suppress the water signal, the number and frequency of scan counts required and the evaluation of the signal-specific quantification of ketone and alcohol groups (Figure S2). Optimal values were found for 32 scans with repetition rates of 15 s at a water suppression level of −50 dB, which allowed quantification with deviations of

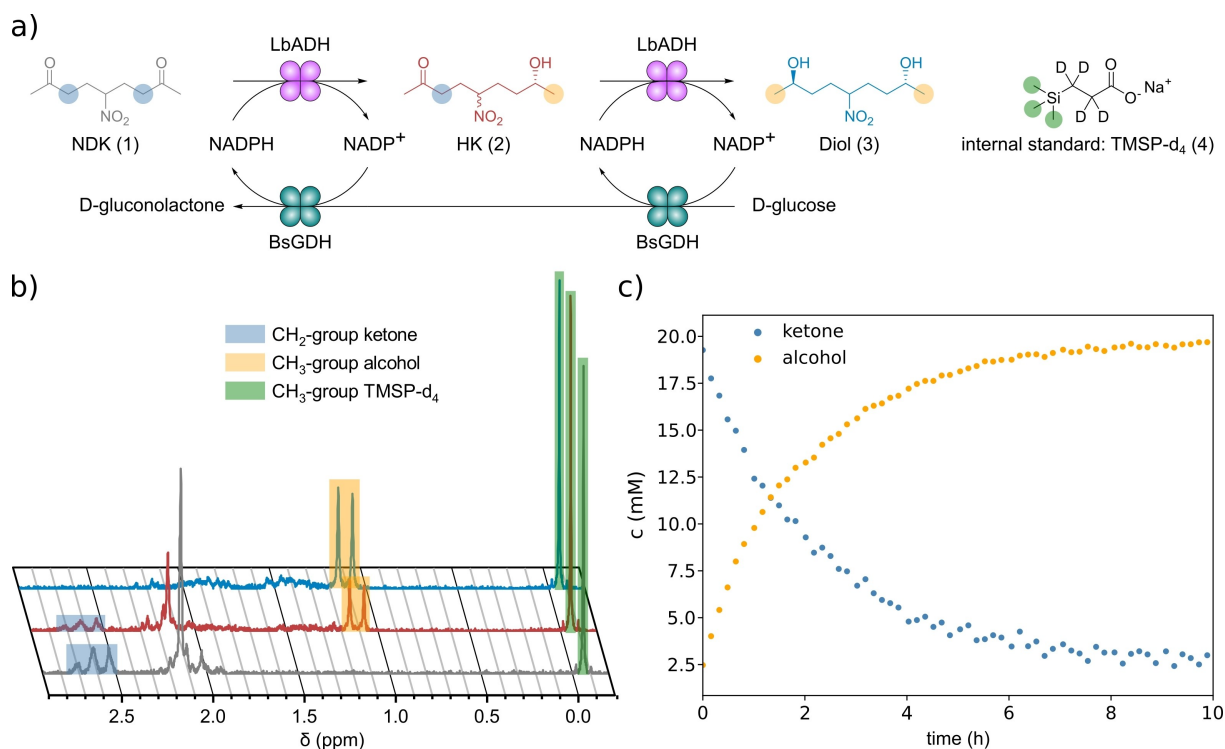


Figure 1. Benchtop NMR-based reaction monitoring; a) Reaction equation of the reduction of NDK catalyzed by the alcohol dehydrogenase LbADH with regeneration of the cofactor NADPH achieved by the oxidation of the sacrificial substrate glucose by the glucose dehydrogenase BsGDH. TMSP-d₄ was used as an internal standard for quantification. Indicative methylene and methyl protons are color-coded; b) Example spectra of NDK (blue), HK (red) and diol (grey) to illustrate the change in monitored signals during the reduction of NDK; c) Batch reaction monitoring of the model reaction within an NMR sample tube.

< 10% and < 15% for concentrations of ketone and alcohol, respectively.

To investigate the suitability of benchtop NMR for the in situ analysis of NDK reduction, we then performed batch experiments with the dissolved enzymes in an NMR tube using standard conditions for the enzymatic reaction (0.7 μM LbADH and 1.9 μM BsGDH, 10 mM 1, 100 mM glucose, in KPi buffer, 26 $^{\circ}\text{C}$).^[20] The ketone and alcohol concentrations were calculated by integrating the signals specified above, normalizing the peak sizes and then comparing them with the internal standard. The control of the NMR measurements and the analysis of the resulting raw data in CSV format were both performed automatically by Python codes, so that only the initial parameters and the signal ranges to be analyzed had to be set by the user. The data in Figure 1c showed an increase in alcohol at a steadily decreasing overall rate, since the rates of the first and second reduction steps of the two carbonyl groups of NDK and HK are the same in the case of LbADH,^[34,37] in contrast to other NADPH-dependent ketoreductases.^[38]

We then proceeded to a microfluidic setup with a continuous flow and inline analysis with benchtop NMR (for details of the laboratory setup, see Figure S3). To test this setup, the two enzymes LbADH and BsGDH were recombinantly expressed as SpyCatcher and SpyTag modified variants, respectively, and introduced into all-enzyme hydrogel (AEH) reactors using the previously described method by self-assembled cross-linking of the two enzymes.^[20] The AEH reactors prepared in this way had a linear reaction channel with a volume of 150 μL and contained approximately 3.0 mg SC-LbADH and 2.3 mg of BsGDH-ST. The reactors were perfused with substrate solution (10 mM NDK in a phosphate buffer, see SI for details) and the effluent was fed directly into the flow cell of the NMR benchtop instrument. Using variable flow regimes, the decrease or increase of ketone or alcohol, respectively, was monitored by inline NMR using the

previously optimized measurement parameters (Figure 2). Representative flow experiments showed a clear dependence on the ketone and alcohol concentration (blue and orange diagrams, respectively, in Figures 2b and c), as expected from the change in contact time of the reactants with the catalytic AEH materials. Verification of the proportions of keto and alcohol groups in the substrate and product, quantified by NMR and cross-validated by HPLC analysis, which also enabled the determination of intermediate HK amounts, showed very good agreement with deviations of less than 5% between the two methods (Figure S4). These initial results indicated that the flow rate is an ideal parameter for adjusting the performance of the reactor reliably and quickly. Further investigations with several changes between alternating flow rates confirmed this reliability (Figure S5), but also indicated a slight instability of the substrate NDK over prolonged storage times (Figure S6). Observation of the different flow profiles also showed that regardless of whether the experiment was started with an initially high or low flow rate (Figures 2b, 2c, S5), a significant loss of reactor performance occurred after about 10 mL. Thereafter, all AEH reactors showed a gradual decrease in catalytic performance over time, which is a major general challenge in the implementation of biocatalysts for industrial processes.^[24] In the case of the reactors used here, the initial losses are likely due to loosely bound AEH material being flushed out of the reactor by the hydrostatic pressure, while the continuous loss of activity in the later stages is due to slower loss of material and/or denaturation of the enzyme, similar as observed in previous studies.^[20–21]

To address the problem of unstable reactor efficiency, we chose a recently developed method to formulate AEH materials as monodisperse foams.^[22] By foaming and drying the self-assembling enzymes, both an increase in the surface area of the crosslinked AEH materials and an improved mechanical stability

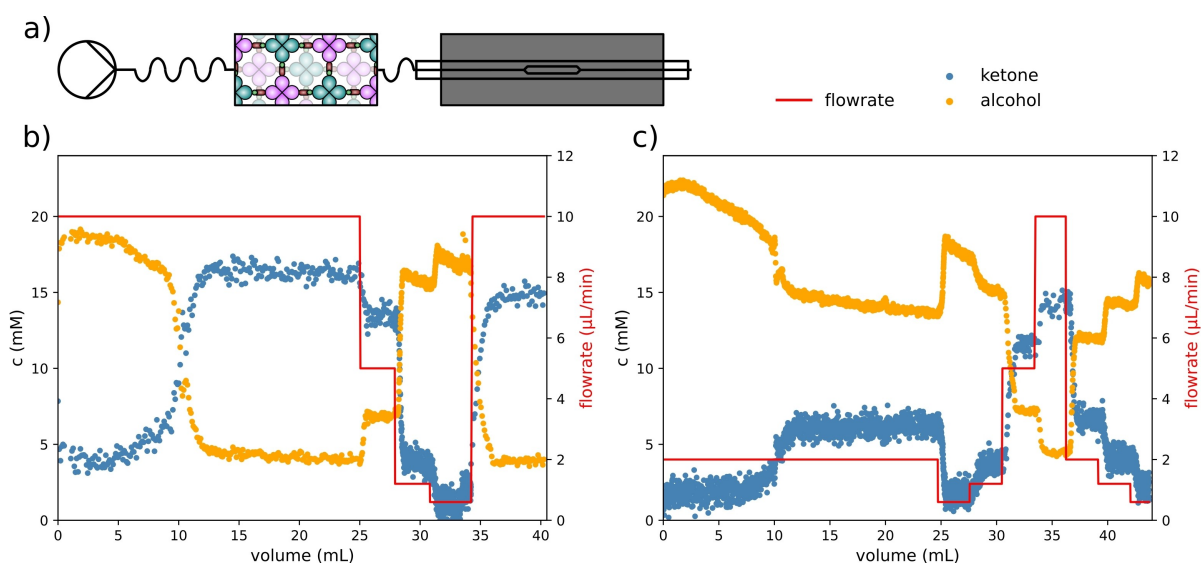


Figure 2. Benchtop NMR-based inline reaction monitoring under continuous flow conditions. a) Schematic of the reaction setup, for a photographic representation see Figure S3; b, c) Representative AEH reactors operated with two different flow regimes where high and low flow rates varied (red lines). Note the dependence of ketone and alcohol concentration (blue and orange graphs, respectively). In both experiments, the reactors lost conversion efficiency after about 10 mL, which could be adjusted by changing the flow rate.

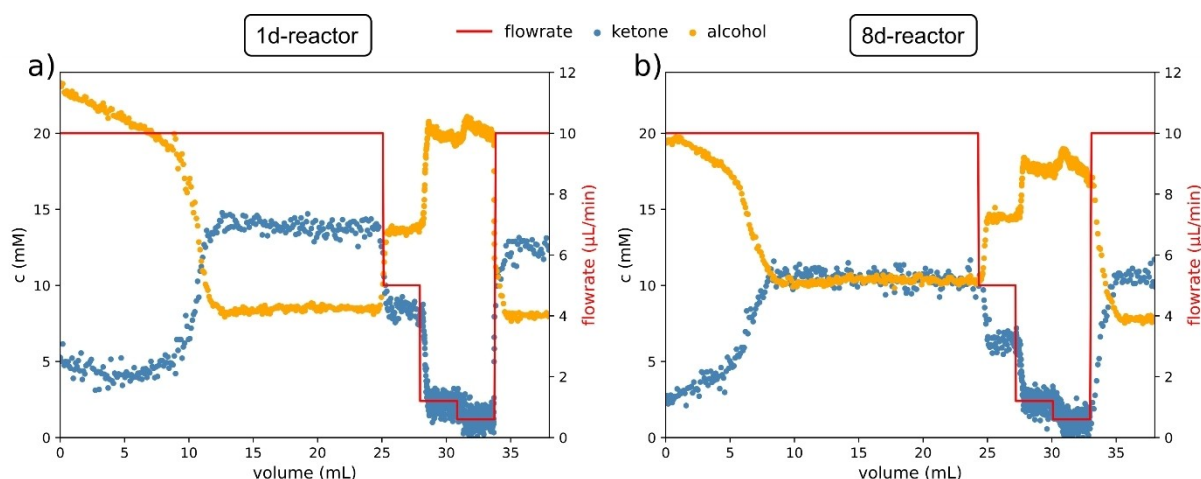


Figure 3. Benchtop NMR-based inline reaction monitoring of micro reactors equipped with AEH foam, dried for either 1 day (a) or 8 days (b). Reagent, flow and NMR conditions were as described above. Note that while both reactors show a drop in performance after 10 mL, they significantly outperform monolithic AEH materials (Figure 2). Additionally, the reactor that underwent longer drying (b) maintained a higher conversion rate even after the performance drop.

and thus resistance to hydrodynamic pressure loads are achieved. To test whether these materials progress under inline NMR control, we first prepared two reactors, each with a volume of 150 μL , filled with AEH foam, which were dried for either 1 day or 8 days to increase the materials' mechanical stability. The reactors were then operated under the previously used flow conditions (Figure 3). The results showed that although the foam reactors exhibited a similar loss in productivity after approximately 10 mL of reaction volume, the foam showed a significantly higher conversion at the same flow rate compared to the previously used monolithic AEH materials (Figure 3a). Prolonged drying of the reactor further increased this stability and also reduced the drop in conversion after about 10 mL reaction volume (Figure 3b).

Although the biocatalytic foam reactors showed a significant improvement in performance, the general problem remained that enzyme reactors do not work consistently efficient over the entire course of the process. In order to get the maximum temporal performance out of a reactor, we therefore wanted to take advantage of the possibilities of inline analytics and dynamically adjust the decisive process parameter of the flow rate via a feedback loop to achieve maximum performance by changing the contact times. Such adaptive control of reactor performance could in principle also be suitable for other reactor concepts and reactions. To implement this approach, a Python-based code was developed to enable automated data acquisition and analysis, as well as direct control of the pumps. To ensure the algorithm is highly accessible, NMR spectra in CSV format were chosen as input, making the code compatible with various instruments beyond the NMR spectrometer used in this study. As shown in the simplified workflow (Figure 4), the code controls the flow rate to achieve a desired product concentration. For this purpose, the relevant ranges are extracted and analyzed from the CSV data, the product concentration is calculated and compared to predefined threshold values that define the desired concentration range. If the actual value is above or below the threshold

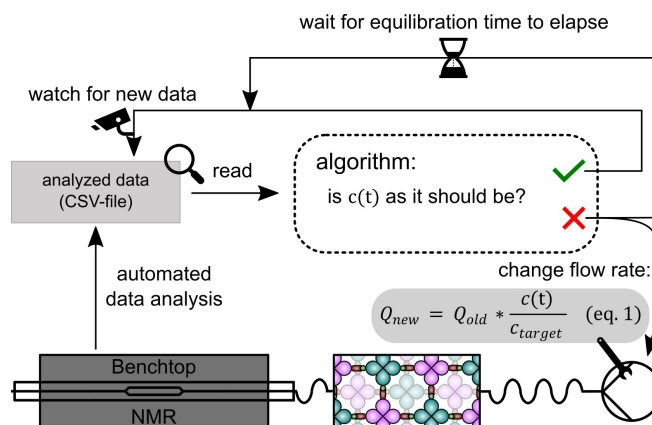


Figure 4. Simplified mode of operation of the algorithm. Q : Volumetric flow rate, $c(t)$: current concentration calculated as average from a user defined number of latest datapoints, c_{target} : target concentration.

values, the flow rate is increased or decreased, respectively. After changing the flow rate, an equilibration phase is observed to account for the system's delay (Figure 4). Although the rules can be adjusted as needed, we chose to have the flow rate change proportionally to the difference between the flow rate and target concentration (eq. 1). For a more comprehensive workflow of the codes and algorithms, see Figure S7.

The functionality of the algorithm was evaluated using NMR to monitor and adjust the behavior of reactors containing foams with different drying times (Figure 5). In the first series of experiments, the target concentration was set at " ≥ 15 mM". In both the less (1 day drying, 1d-reactor, Figure 5a) and the more productive reactor (8 days drying, 8d-reactor, Figure 5b), the initial conversions were above the threshold value, as expected from the earlier experiments (Figure 3). When the conversion in the 1d-reactor dropped below 15 mM, the algorithm initially reduced the flow rate only slightly, as the target value was only slightly undershot. As the conversion fell further, larger adjustments were automatically made, which led to an increase in

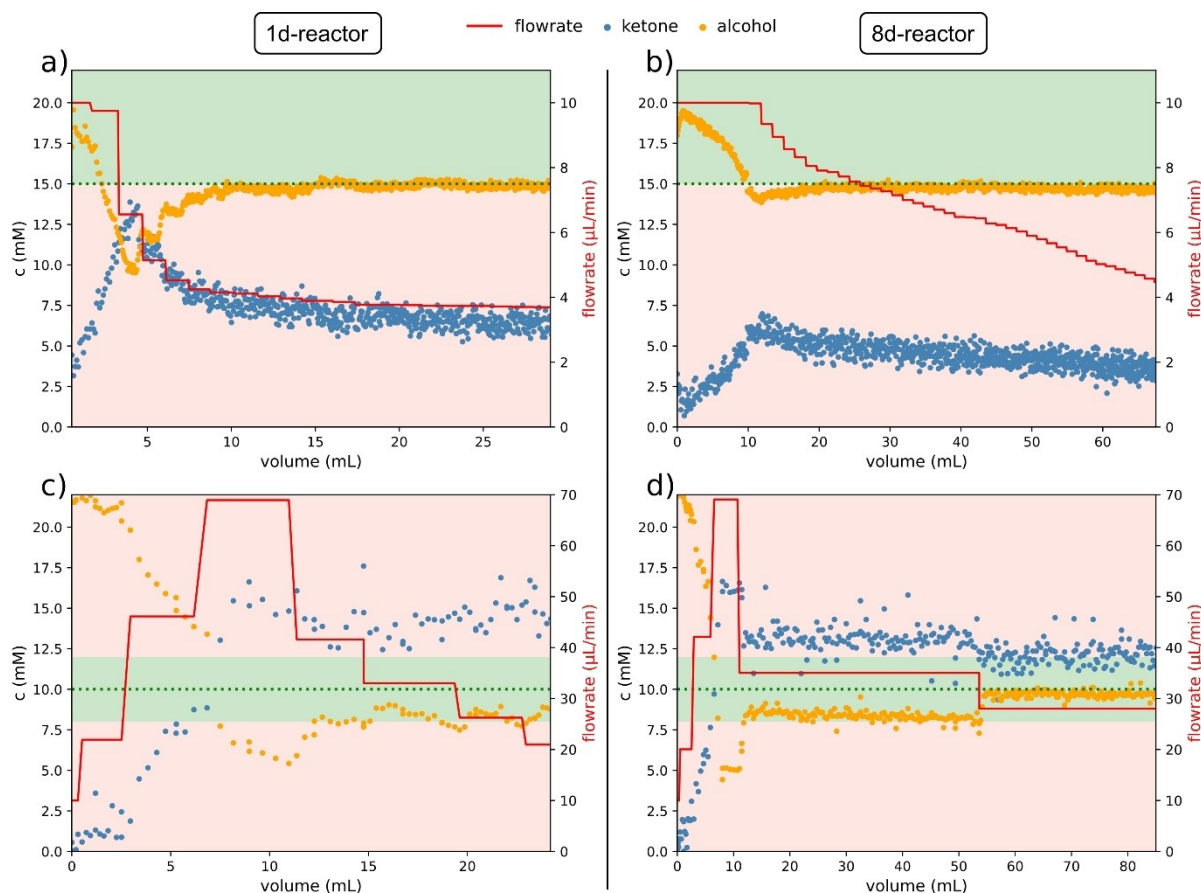


Figure 5. Realization of constant biocatalysis processes by inline NMR reaction monitoring with automatic adjustment of the flow rate. Two differently prepared and thus differently stable biocatalytic foam reactors that had been dried for either 1 day or 8 days (1d-reactor and 8d-reactor, in Figures 5a, c and 5b, d, respectively) were operated under inline NMR reaction monitoring with automatic adjustment of the flow rate to ensure a process with product concentrations of ≥ 15 mM (Figures 5a, b) or 10 ± 2 mM (Figures 5c, d). The range defined by the threshold values is highlighted in green, the concentrations of ketone and alcohol are indicated by blue and orange measuring points respectively and the automatically adjusted flow rate is shown as a red graph.

product, but did not yet reach the target 15 mM. Successive further adjustments after the equilibration phase led to the target value being reached, which could then be maintained throughout the rest of the process. This result showed that the initial drop in reactor performance was too fast to be fully compensated by the algorithm, but that the slow decay phase was fully compensable. The more stable 8d-reactor did not fall below the threshold value until later and to a lesser extent, so that it could be maintained practically throughout the entire process (Figure 5b). In further experiments, similar 1d- and an 8d-reactors were used to achieve a constant product concentration of 10 ± 2 mM (Figures 5c and 5d, respectively). Since the initial flow rate of $10 \mu\text{L}/\text{min}$ led to higher product concentrations as expected, the flow rates were automatically increased in several steps so that maximum values of almost $70 \mu\text{L}/\text{min}$ were set in both cases, which were subsequently lowered again to reach the target value. Even though more adjustments were required for the 1d-reactor than for the more stable 8d-reactor, the algorithm was able to run the processes at a constant productivity in both cases. These results clearly demonstrated that inline NMR reaction monitoring can be utilized for automated pump control, enabling the implementa-

tion of consistent biocatalysis processes through automatic data analysis integration. We were also able to show that by fine-tuning the control code to take into account a more sensitive control response and the self-decomposition of the NDK substrate, an 8d foam reactor could be operated with maximum productivity over the entire process time of > 13 d (Figure S8). Hence, the approach demonstrated here can also be used for the economic optimization of biocatalysis processes, as maximum high conversion rates should usually be achieved over the entire service life of the reactor.

Conclusions

In summary, we have demonstrated for the first time that constant biocatalysis processes can be achieved through inline NMR reaction monitoring by automatically evaluating acquired data and adjusting critical process parameters accordingly. The use of a benchtop NMR instrument for the autonomous improvement of biocatalytic synthesis of chiral alcohols effectively addresses the significant challenge of declining reactor efficiency over extended process durations. While this study

focused on adjusting the flow rate, the developed framework is designed to enable autonomous experimentation and productivity optimization based on arbitrary other parameters such as temperature, buffer conditions, small-molecule additives, or the activity of alternative enzyme variants. We are confident that the concept and methodology developed in this proof-of-concept will provide a significant impetus for future innovations in precision biocatalysis.

Supporting Information

The authors have cited additional references within the Supporting Information.^[39–40] The software used in this publication and an example dataset are publicly available.

Acknowledgments

This work was financially supported through the Helmholtz Association program “Materials Systems Engineering” under the topic “Adaptive and Bioinstructive Materials Systems”.

We thank Benjamin Zagoruiko, Franziska Seiz, Manideep Jayavarapu, Minh Hieu Nguyen and Nico Henkenhaf for their work on the analysis and control software. We also thank our colleagues at IBG-1 for help with protein production and T. Rinesch and F. Siepel (both Magritek GmbH) for their technical support with the benchtop NMR.

Conflict of Interests

The authors declare no conflict of interest.

Keywords: Biocatalysis · Microfluidics · Automation · Open-Source · Inline benchtop NMR

- [1] A. D. Clayton, *Chem. Methods* **2023**, 3, e202300021.
- [2] A. I. Leonov, A. J. S. Hammer, S. Lach, S. H. M. Mehr, D. Caramelli, D. Angelone, A. Khan, S. O'Sullivan, M. Craven, L. Wilbraham, L. Cronin, *Nat. Commun.* **2024**, 15, 1240.
- [3] C. J. Taylor, A. Pomberger, K. C. Felton, R. Grainger, M. Barecka, T. W. Chamberlain, R. A. Bourne, C. N. Johnson, A. A. Lapkin, *Chem. Rev.* **2023**, 123, 3089–3126.
- [4] S. V. Ley, D. E. Fitzpatrick, R. J. Ingham, R. M. Myers, *Angew. Chem. Int. Ed. Engl.* **2015**, 54, 3449–3464.
- [5] S. V. Ley, D. E. Fitzpatrick, R. M. Myers, C. Battilocchio, R. J. Ingham, *Angew. Chem. Int. Ed.* **2015**, 54, 10122–10136.
- [6] L. Capaldo, Z. Wen, T. Noël, *Chem. Sci.* **2023**, 14, 4230–4247.
- [7] P. J. Nieuwenhuizen, D. Lyon, *J. Commer.* **2011**, 17, 159–164.
- [8] B. Hauer, *ACS Catal.* **2020**, 10, 8418–8427.
- [9] S. Wu, R. Snajdrova, J. C. Moore, K. Baldenius, U. T. Bornscheuer, *Angew. Chem. Int. Ed.* **2021**, 60, 88–119.
- [10] E. L. Bell, W. Finnigan, S. P. France, A. P. Green, M. A. Hayes, L. J. Hepworth, S. L. Lovelock, H. Niikura, S. Osuna, E. Romero, K. S. Ryan, N. J. Turner, S. L. Flitsch, *Nat. Rev. Methods Primers* **2021**, 1, 46.
- [11] R. A. Sheldon, J. M. Woodley, *Chem. Rev.* **2017**, 118, 801–838.
- [12] B. Wiltschi, T. Cernava, A. Dennig, M. Galindo Casas, M. Geier, S. Gruber, M. Haberbauer, P. Heidinger, E. Herrero Acero, R. Kratzer, C. Luley-Goeidl, C. A. Müller, J. Pitzer, D. Ribitsch, M. Sauer, K. Schmölder, W. Schnitzhofer, C. W. Sensen, J. Soh, K. Steiner, C. K. Winkler, M. Winkler, T. Wriessneger, *Biotechnol. Adv.* **2020**, 38, 107520.
- [13] J. M. Woodley, *Appl. Microbiol. Biotechnol.* **2019**, 103, 4733–4739.
- [14] A. Kuchler, M. Yoshimoto, S. Luginbuhl, F. Mavelli, P. Walde, *Nat. Nanotechnol.* **2016**, 11, 409–420.
- [15] S. P. France, L. J. Hepworth, N. J. Turner, S. L. Flitsch, *ACS Catal.* **2017**, 7, 710–724.
- [16] K. S. Rabe, J. Muller, M. Skoupi, C. M. Niemeyer, *Angew. Chem. Int. Ed.* **2017**, 56, 13574–13589.
- [17] J. Britton, S. Majumdar, G. A. Weiss, *Chem. Soc. Rev.* **2018**, 47, 5891–5918.
- [18] L. L. Martin, T. Peschke, F. Venturoni, S. Mostarda, *Curr. Opin. Green Sustain. Chem.* **2020**, 25.
- [19] M. Crotti, M. S. Robescu, J. M. Bolivar, D. Ubiali, L. Wilson, M. L. Contente, *Front. Catal.* **2023**, 3.
- [20] T. Peschke, P. Bitterwolf, S. Gallus, Y. Hu, C. Oelschlaeger, N. Willenbacher, K. S. Rabe, C. M. Niemeyer, *Angew. Chem. Int. Ed.* **2018**, 57, 17028–17032.
- [21] P. Bitterwolf, S. Gallus, T. Peschke, E. Mittmann, C. Oelschlaeger, N. Willenbacher, K. S. Rabe, C. M. Niemeyer, *Chem. Sci.* **2019**, 10, 9752–9757.
- [22] J. S. Hertel, P. Bitterwolf, S. Kröll, A. Winterhalter, A. J. Weber, M. Grösche, L. B. Walkowsky, S. Heißler, M. Schwotzer, C. Wöll, T. van de Kamp, M. Zuber, T. Baumbach, K. S. Rabe, C. M. Niemeyer, *Adv. Mater.* **2023**, 35, 2303952.
- [23] P. De Santis, L.-E. Meyer, S. Kara, *React. Chem. Eng.* **2020**, 5, 2155–2184.
- [24] P. Žnidaršič-Plazl, *Curr. Opin. Green Sustain. Chem.* **2021**, 32, 100546.
- [25] E. Calleri, C. Temporini, R. Colombo, S. Tengattini, F. Rinaldi, G. Brusotti, S. Furlanetto, G. Massolini, *TrAC Trends Anal. Chem.* **2021**, 143, 116348.
- [26] M. Grootveld, B. Percival, M. Gibson, Y. Osman, M. Edgar, M. Molinari, M. L. Mather, F. Casanova, P. B. Wilson, *Anal. Chim. Acta* **2019**, 1067, 11–30.
- [27] P. Giraudeau, F.-X. Felpin, *React. Chem. Eng.* **2018**, 3, 399–413.
- [28] T. Maschmeyer, D. J. Russell, J. G. Napolitano, J. E. Hein, *Magn. Reson. Chem.* **2024**, 62, 310–322.
- [29] P. Sagmeister, F. F. Ort, C. E. Jusner, D. Hebrault, T. Tampone, F. G. Buono, J. D. Williams, C. O. Kappe, *Adv. Sci.* **2022**, 9, 2105547.
- [30] K. A. Farley, U. Reilly, D. P. Anderson, B. P. Boscoe, M. W. Bundesmann, D. A. Foley, M. S. Lall, C. Li, M. R. Reese, J. Yan, *Magn. Reson. Chem.* **2017**, 55, 348–354.
- [31] R. Legner, A. Wirtz, M. Jaeger, *J. Spectrosc.* **2018**, 2018, 5120789.
- [32] C. Claaßen, K. Mack, D. Rother, *ChemCatChem* **2020**, 12, 1190–1199.
- [33] L. F. Schmidt, L. Jolly, L. Hennecke, F. Lopez Haro, H. Gröger, A. Liese, *Org. Process Res. Dev.* **2024**, 28, 3791–3800.
- [34] M. Skoupi, C. Vaxelaire, C. Strohmann, M. Christmann, C. M. Niemeyer, *Chem. Eur. J.* **2015**, 21, 8701–8705.
- [35] S. Kröll, T. Burgahn, K. S. Rabe, M. Franzreb, C. M. Niemeyer, *Small* **2023**, 2304578.
- [36] L. Sellés Vidal, C. L. Kelly, P. M. Mordaka, J. T. Heap, *Biochim. Biophys. Acta Proteins Proteomics* **2018**, 1866, 327–347.
- [37] P. Bitterwolf, A. E. Zoheir, J. Hertel, S. Kröll, K. S. Rabe, C. M. Niemeyer, *Chem. Eur. J.* **2022**, 28, e202202157.
- [38] F. Ott, K. S. Rabe, C. M. Niemeyer, G. Gygli, *ACS Catal.* **2021**, 11, 10695–10704.
- [39] S. H. Hansen, T. Kabbeck, C. P. Radtke, S. Krause, E. Krolitzki, T. Peschke, J. Gasmi, K. S. Rabe, M. Wagner, H. Horn, J. Hubbuch, J. Gescher, C. M. Niemeyer, *Sci. Rep.* **2019**, 9, 8933.
- [40] N. Mehendale, F. Jenne, C. Joshi, S. Sharma, S. K. Masakapalli, N. MacKinnon, *Molecules* **2020**, 25, 4675.

Manuscript received: October 9, 2024

Version of record online: ■■, ■■